Magnetic behavior of one- and two-dimensional nanostructures stabilized by surface-state electrons: a kinetic Monte Carlo study

A S Smirnov[1,2]**, N N Negulyaev**[1,4]**, W Hergert**[1]**, A M Saletsky**[2] **and V S Stepanyuk**[3]

[1] Fachbereich Physik, Martin-Luther-Universität, Halle-Wittenberg, Friedemann-Bach-Platz 6, D-06099 Halle, Germany
[2] Faculty of Physics, Moscow State University, 119899 Moscow, Russia
[3] Max-Planck-Institut für Mikrostrukturphysik, Weinberg 2, D-06120 Halle, Germany
E-mail: negulyaev@mpi-halle.mpg.de

Abstract. Recent experiments have demonstrated that it is possible to create macroscopic-ordered one- and two-dimensional nanostructures on (111) noble metal surfaces exploiting long-range substrate-mediated interaction. Here, we report on the systematic theoretical studies of magnetic properties of these atomic structures in the externally applied magnetic field. The spin dynamics is investigated by means of the kinetic Monte Carlo method based on transition-state theory. For the characteristic values of (i) magnetic anisotropy energy of adatoms and (ii) exchange coupling between adatoms in the considered class of nanostructures, we reveal the hysteresis-like behavior at low temperatures (typically at 1–3 K).

Contents

[4] Author to whom any correspondence should be addressed.

TH-2009-14

**IOP** Institute of Physics Φ DEUTSCHE PHYSIKALISCHE GESELLSCHAFT

1. Introduction

Modern nanoscience manifests strong interest in magnetic nanostructures on surfaces. It is believed that such systems can be of great importance for the development of advanced atomic-scale magnetic devices [1, 2]. Magnetic nanostructures on metal substrates attract significant attention due to the enhanced magnetic moments of low-coordinated adatoms [3]–[5] and the large magnetic anisotropy energy (MAE) peculiar to a magnetic unit [6]–[9]. When the amount of thermal energy, which causes fluctuation of the magnetic moment, is enough to overcome the MAE barrier, the spin orientation is random. This takes place at the so-called blocking temperature [10, 11]. In real magnetic ensembles, interaction between individual spins (exchange interaction, dipole–dipole interaction, and indirect exchange interaction through the substrate) could stabilize ferromagnetic (FM) order, leading to higher blocking temperatures [10]–[12]. Up to now, numerous experimental and theoretical studies have revealed a lot of nanoscale systems exhibiting hysteresis-like (i.e. FM) behavior: quasi-1D (one-dimensional) stripes [13]–[17], monatomic wires [10], [17]–[21], pillars [22], nanodots [23]–[27], nanoscale clusters and islands [28]–[30].

Recent studies on low-temperature self-assembly of metal adatoms on (111) metal substrates have demonstrated the existence of a new class of 1D and 2D systems: nanostructures of individual adatoms stabilized by the long-range substrate-mediated interaction (LRI) [31]–[33]. It is well known that conduction electrons on a (111) noble metal surface form a 2D nearly free electron gas confined in the vicinity of the top layer. Scattering of the surface states at adatoms (or defects) leads to the standing wave patterns of local density of states [34]–[42] and to indirect oscillating interaction between adsorbates [31]–[33]. On surfaces supporting the surface-state electrons the LRI decays as $1/r^2$ (where r is the interatomic distance) and oscillates with a period of $\lambda_F/2$ (where λ_F is a surface-state Fermi wavelength) [43].

If two adatoms are separated by the first nearest neighbor (NN) distance r_0 (figure 1) the interaction is determined only by the short-range chemical bonding, and it is strongly attractive. At larger interatomic distances ($> 5\,\text{Å}$) the interplay between adatoms is caused by the elastic interaction [44, 45] and the substrate-mediated LRI. The schematic description of the 'adatom–adatom' LRI is presented in figure 1. There is a repulsive barrier A; its magnitude is between 10 and 60 meV, depending on the sort of interacting adatoms and the type of surface [41], [46]–[52]. At low temperatures ($< 50\,\text{K}$) this repulsive barrier inhibits agglomeration of two adatoms into a dimer, decreasing the probability of cluster formation. At larger separations (see figure 1) there is an attractive minimum B; its magnitude is a few meV [41, 46, 47], [52]–[54]. Typically, this minimum is located at separations which are 5–10 times larger than the NN distance r_0. For instance, on Cu(111) the position of the minimum B is at 12 Å [41, 46, 47, 54], while on Ag(111) it is at 30 Å [52, 53]. There is yet another repulsive barrier C, whose magnitude is usually less than 1 meV. According to [33], at larger separations r, $E(r) \sim \sin(\alpha_1 r + \alpha_2)/r^2$. The positions of the minima and maxima of the LRI potential (figure 1) are determined by the type of surface and scattering properties of adatoms.

Several theoretical and experimental investigations have demonstrated that one can create macroscopic-ordered 1D and 2D nanostructures exploiting atomic self-assembly promoted by surface-state electrons. Dilute 2D nanoislands of individual adatoms stabilized by the LRI have been observed experimentally [46, 47] and studied theoretically [55, 56]. It has been found that cerium adatoms randomly deposited on Ag(111) form a perfectly ordered 2D superlattice [52, 53, 57, 58] (figure 2(a)) (for Cs on Ag(111) see [59]). One can exploit stepped surfaces [60]
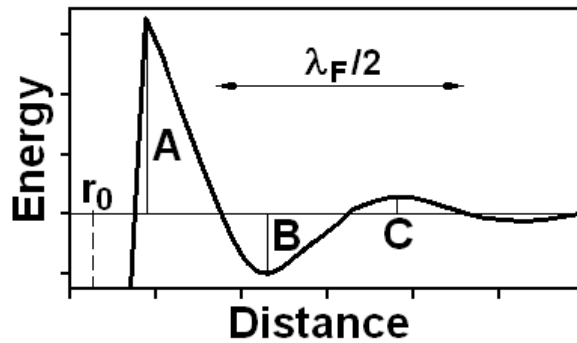
Figure 1. Schematic description of the LRI energy between two adatoms on a (111) noble metal surface supporting 2D free electron gas. Repulsive barriers A and C and attractive minimum B are marked. Distance r_0 corresponds to the NN separation between the adatoms.

(a)

(b)
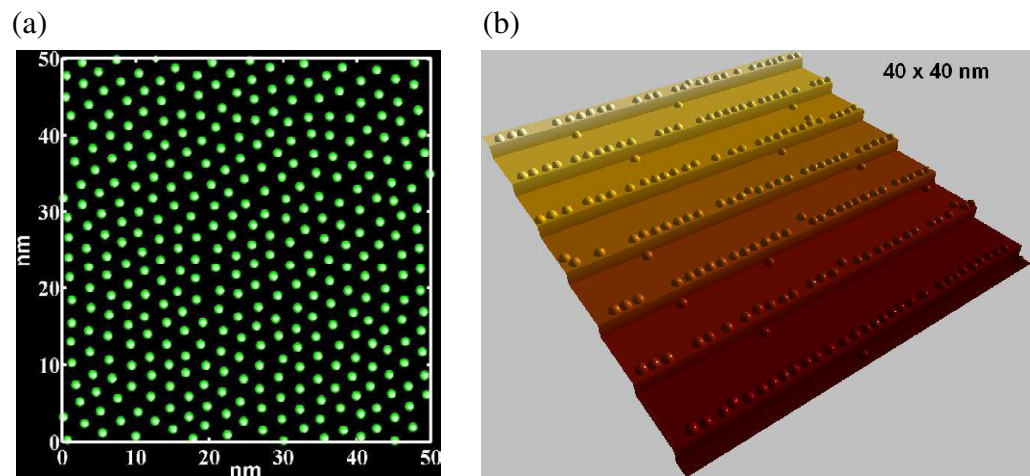
Figure 2. Nanostructures of individual adatoms stabilized by the substrate-mediated LRI. (a) Superlattice of Ce adatoms on Ag(111) [52, 53, 58], (b) monatomic Fe wires in the vicinity of descending Cu(111) steps [60]. The interatomic separation in these nanostructures corresponds to the position of the first local minimum B in the 'adatom–adatom' LRI potential (figure 1).

(figure 2(b)), molecular templates [61] or reconstructed substrates [62] for self-organization of 1D atomic structures. The separation between adatoms in all these nanostructures corresponds to the position of the local minimum B in the LRI potential (figure 1). While the details of the growth of 1D and 2D nanostructures stabilized by surface-state electrons are well understood to date, the knowledge of their magnetic properties has still not been gained.

The goal of this paper is to perform theoretical studies of magnetic properties of the 1D and 2D nanostructures stabilized by indirect LRI between adatoms on (111) metal surfaces. We demonstrate that in the externally applied magnetic field at low temperatures (typically at 1–3 K) such systems could exhibit hysteresis-like (i.e. FM) behavior promoted by the indirect exchange coupling between adatoms through the substrate. We reveal how the coercive field depends on the magnitude of exchange interaction between adatoms and on the MAE of individual adatoms
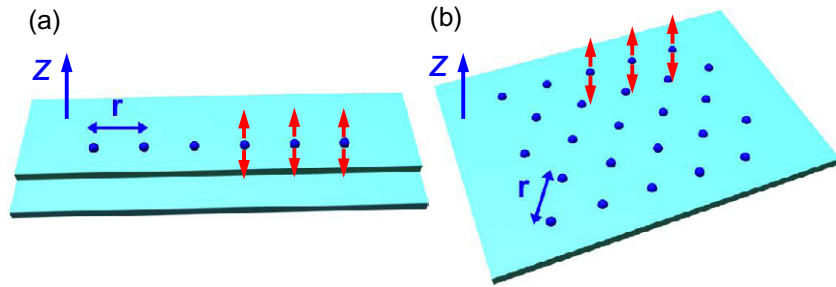
Figure 3. A schematic view of two systems considered within our study: (a) finite 1D chain of equidistantly separated spins and (b) 2D hexagonal-ordered array of equidistantly separated spins. We suppose that both systems represent atomic structures stabilized by the substrate-mediated LRI (figure 2). The easy magnetization axis of an individual adatom is considered to be collinear to the vector Z. Spin orientations along and opposite to the easy axis are demonstrated using red arrows.

within a nanostructure. We study the dependence of the magnetization response on the size of a system (number of adatoms in a nanostructure). As a method of investigation, we employ the kinetic Monte Carlo (kMC) model for simulation of spin dynamics [19].

The remainder of the paper is organized as follows. In section 2, we give the details of the model that was used to simulate the spin dynamics. In section 3, we present the results of our calculations and discuss them.

2. The model

In this section, we describe the model that was utilized to simulate spin dynamics and we discuss the parameters of the investigated systems.

Two different systems are considered. The first system is a 1D finite chain of spins (figure 3(a)), which represents a monatomic wire of magnetic adatoms stabilized by the LRI in the vicinity of a descending step (figure 2(b)) [60] or inside a molecular trench [61]. Since the average distance between the wires is several times larger than the interatomic distance within a wire [60, 61], the effect of interchain exchange interaction on the magnetization response can be neglected. The second system under study is a 2D hexagonal-ordered array of spins (figure 3(b)), which represents magnetic adatoms assembled in a hexagonal nanoisland [46, 47] or superlattice [52, 53, 57, 58] (if the number of adatoms tends to infinity (figure 2(a))). For both systems the Hamiltonian of the classical Heisenberg model with an on-site anisotropy and external magnetic field $\vec{B}$ can be written as [19]

$$H = J \sum_{\langle i,j \rangle} \vec{s}_i \vec{s}_j - K \sum_i (s_{z,i})^2 - \mu \vec{B} \sum_i \vec{s}_i, \tag{1}$$

where $\vec{s}_i$ is the normalized spin value at site i, $s_{z,i}$ is the Z-component of the vector $\vec{s}_i$ (see the direction definition in figure 3), the summation $\langle i,j \rangle$ is taken over all neighboring pairs of spins i and j, $\vec{s}_i \vec{s}_j$ is a scalar product of spins at sites i and j. J is the exchange coupling constant ($J < 0$ for FM and $J > 0$ for antiferromagnetic (AFM) interaction), K is the MAE and μ is

the magnetic moment of an adatom. Individual spin is considered as a classical variable. In our study we concentrate on the FM-coupled spins only.

The parameters of the Hamiltonian (1) are taken from our *ab initio* calculations. Density function theory reveals that the typical magnitude of the surface-state-mediated exchange interaction between magnetic adatoms is about 0.1–0.5 meV [54], when the 'adatom–adatom' separation corresponds to the position of the local minimum B in the LRI potential (figure 1). Depending on the sort of adatoms, this interaction can be either FM or AFM[5]. Within our study we consider that $|J|$ is in the interval from 0 to 1 meV ($J < 0$), which implies a reasonable range of possible values of exchange coupling between the neighboring adatoms (figure 3). The magnitude of the MAE K of an adatom in a chain (figure 3(a)) and in a 2D hexagonal-ordered array (figure 3(b)) is very close to the MAE of a single adatom on a clean substrate, since the separation between spins is a few times larger than the NN distance r_0. Typically, the magnitude of K of a magnetic adatom on a metal surface is about 1.0 meV [64]. However, in some cases this value can be strongly enhanced. For instance, MAE of an individual Co adatom on Pt(111) is 9.3 meV [6]. Thus, within our study we consider that K varies from 0.1 to 10 meV. The magnetic moment of an adatom is taken to be $3.2\mu_B$ ($\mu_B \approx 0.058$ meV T^{-1} is the Bohr magneton), which corresponds to the magnetic moment of a single iron adatom on Cu(111) [65, 66]. The easy magnetization axis is considered to be perpendicular to the surface plane, i.e. collinear to the direction of the vector Z (figure 3).

We analyze the magnetization response for nanostructures shown on figures 3(a) and (b) to the externally applied magnetic field applied along the easy magnetization axis. We start from a strong field $-B_0$ (-5 T), oriented along the $-Z$-direction, at which all spin magnetic moments are aligned along the $-Z$-direction. The field strength increases by an increment $\Delta B = 0.001$ T gradually to $+B_0$ (5 T), which corresponds to the situation when the magnetic field is oriented along the Z-direction. Then the field decreases back to $-B_0$, so that a sweeping cycle is complete. We consider that the magnitude of the sweeping rate of the external magnetic field dB/dt is about 130 T s^{-1} [19]. We use free boundary conditions in our simulations. Spin–spin correlation in open 1D chains and 2D hexagonal arrays is drastically reduced at the border sites [67]. This significantly alters the magnetization reversal rate of the systems, leading to lower blocking temperatures than in the case of periodic boundary conditions.

Diffusion barriers during a single spin flip must be taken into account in order to describe spin dynamics in the investigated systems. In order to do this, we employ the kMC model recently introduced by Li and Liu [19]. This model has been successfully applied for the simulations of the magnetization response of monatomic Co chains on a stepped Pt(997) surface at different temperatures [19]. An individual spin i takes any value between -1 and $+1$ ($s_i = -1/+1$ correspond to the spin orientation along the $-Z/Z$-direction, respectively). If model parameters J and K satisfy the condition $2K > |h_i|$ (where $h_i = (\sum_j J_{ij}s_j + \mu B)s_i$), the energy increment during spin rotation to the opposite direction (from $s_i = -1$ to $+1$ or from $s_i = +1$ to -1) yields a transition-state barrier [19]:

$$\Delta E_i = (2K + h_i)^2/4K. \tag{2}$$

The rate of the single spin flip is calculated then according to the Arrhenius law:

$$v = v_0 \exp(-\Delta E_i/k_B T), \tag{3}$$

---

[5] The results of calculations performed in [54] indicate that for interatomic separation of 12 Å for Ti, V, Cr and Ni pairs, the magnetic coupling mediated by surface-state electrons is ferromagnetic, whereas for Mn, Fe and Co pairs antiferromagnetic states are more stable.
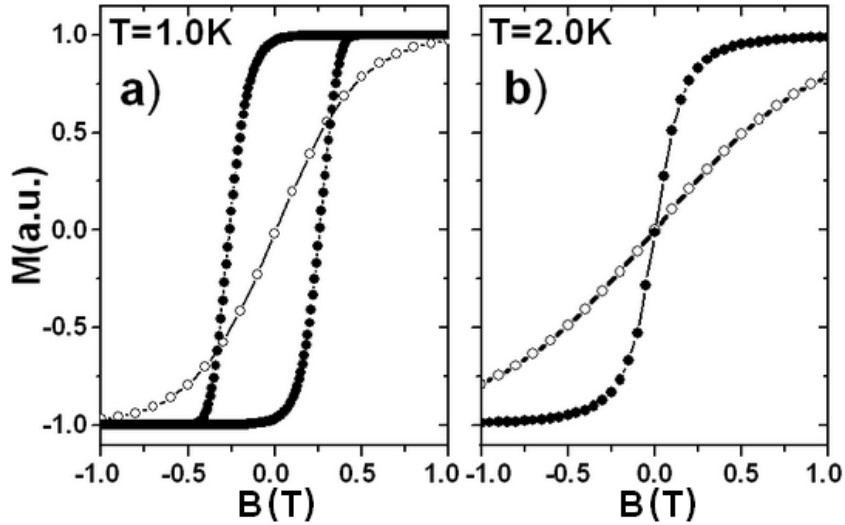
Figure 4. Magnetization response to the external magnetic field for the 1D chain of $N = 100$ spins at two temperatures: (a) 1.0 K and (b) 2.0 K. Black circles correspond to the following values of parameters of the Hamiltonian (1): $K = 1.0$ meV, $J = -0.3$ meV and $\mu = 3.2\mu_B$, while white circles correspond to: $K = 1.0$ meV, $J = 0$ meV and $\mu = 3.2\mu_B$.

where k_B is the Boltzmann constant and prefactor v_0 is 10^9 Hz [10, 19]. If the condition $2K \leqslant |h_i|$ is satisfied, there is no transition state barrier for the spin reversal process, and the Glauber method [68] is used to compute the exponential factor of the rates, with the prefactor to be the same.

If the total number of spins in a system is equal to N, then for every kMC step N different spin flips with the rates $v_1, v_2, \ldots, v_N$ are possible. The time increment τ corresponding to one step of the kMC algorithm is computed using the formulae [63]:

$$\tau = -\ln U \Big/ \sum_{i=1}^{N} v_i, \tag{4}$$

where U is a randomly distributed number in the interval (0, 1).

3. Results and discussion

We start this section with the investigation of the magnetization response for a 1D chain of spins (figure 3(a)).

Figure 4 demonstrates the magnetization response for a chain (figure 3(a)) consisting of $N = 100$ spins at two temperatures: 1.0 K (figure 4(a), black circles) and 2.0 K (figure 4(b), black circles). During simulations we have considered that $J = -0.3$ meV and $K = 1.0$ meV. At the lower temperature the system exhibits hysteresis-like (FM) behavior, while at the higher temperature no hysteresis loop is observed. The hysteresis loop is characterized by the critical magnetic field B_c at which the magnetization is zero. The magnitude of coercive field B_c at $T = 1.0$ K is 0.26 T. While the exchange coupling constant between spins is relatively small ($J = -0.3$ meV), the exchange interaction is the dominant factor responsible for the observed
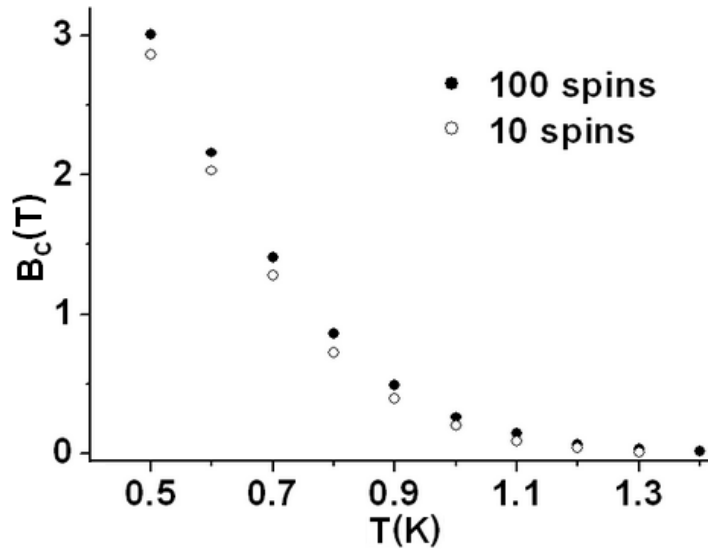
Figure 5. Temperature dependence of coercive field B_c for the 1D chains of $N = 10$ and 100 spins. The parameters of the Hamiltonian (1) are: $K = 1.0$ meV, $J = -0.3$ meV and $\mu = 3.2\mu_B$.

FM behavior at 1.0 K. In order to prove this statement we have simulated the magnetization response for the chain of $N = 100$ non-interacting spins (i.e. $J = 0$ meV). The result for 1.0 K is demonstrated in figure 4(a) (white circles) and for 2.0 K in figure 4(b) (white circles): the system of non-interacting spins has paramagnetic behavior.

It is interesting to study how the coercive field B_c depends on the length of a chain. The results in figure 5 demonstrate a size effect: the temperature dependence of B_c for chains consisting of $N = 100$ (black circles) and $N = 10$ spins (white circles). In both cases, 1D chains exhibit FM behavior up to about 1.5 K. One can see that the size effect is quite weak: increasing the length of the chain by ten times increases B_c by less than 10%. The typical values of coercive field B_c in the studied systems are of the same order as in 1D Co wires grown on Pt(997) [10, 19].

Figure 6 demonstrates the dependence of coercive field B_c for the chain of $N = 100$ spins on the MAE K and exchange constant J. The temperature of the system is $T = 0.5$ K. From figure 6 one can see the onset of ferromagnetism in the whole range of values J and K considered in our study. Increasing J at a fixed K leads to an increase of B_c. Similarly, at a fixed J, larger values of B_c are reached at larger K. We note that we cannot determine B_c for $K > 1.5$ meV, since there are no spin flips within the half-period of oscillations of the externally applied magnetic field: spins keep their initial magnetization fixed along the $-Z$-direction[6].

B_c depends on the value of the sweeping rate dB/dt. Our systematic studies demonstrate that B_c increases monotonically with increasing dB/dt at fixed N, J, K.

Now we turn to the discussion of the magnetization response for a 2D hexagonal-ordered array of spins (figure 3(b)).

---

[6] The half-period of oscillations of the externally applied magnetic field $T_{osc} = 10$ T/130 T s$^{-1} \sim 0.08$ s. On the other hand, at $K = 1.5$ meV, the average time of a single spin flip can be estimated using the formula (2) (see text) $t_{flip} \sim 1/v_0 \exp(((K - 0.5\mu B_0)^2)/(Kk_BT))$ ($\mu = 3.2 * 0.058$ meV T^{-1}, $k_B = 0.086$ meV K^{-1}, $v_0 = 10^9$ Hz, $T = 0.5$ K, $B_0 = 4.5$ T) and is equal to $t_{flip} \sim 0.08$ s. At larger K, $t_{flip} > T_{osc}$, therefore no spin flips are possible.
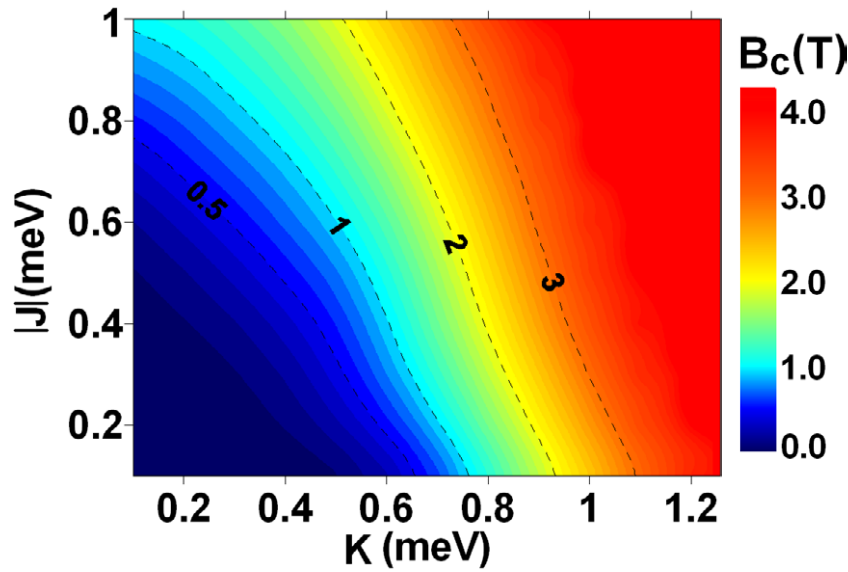
Figure 6. Dependence of coercive field B_c for the chain of $N = 100$ spins on the MAE K and the exchange coupling constant $|J|$ ($J < 0$). The diagram is obtained for $T = 0.5$ K. Dashed curves represent the equipotential lines of coercive field B_c of the corresponding magnitude (see thermometer).

Figure 7 demonstrates the magnetization response of a 2D hexagonal-ordered array (figure 3(b)) consisting of $N = 100$ spins at two temperatures: 1.2 K (figure 7(a), black circles) and 5.0 K (figure 7(b), black circles). During our simulations we have used the following values of parameters in the Hamiltonian (1): $J = -0.3$ meV, $K = 1.0$ meV. At 1.2 K the system exhibits FM behavior, while at 5.0 K the paramagnetic response is observed. The magnitude of B_c at 1.2 K is 0.96 T. FM behavior (figure 7(a)) is promoted mainly by the exchange interaction between spins. We have computed the magnetization response for a 2D array of $N = 100$ non-interacting spins ($J = 0$ meV). The result for 1.2 K is demonstrated in figure 7(a) (white circles): the signal is paramagnetic.

Figure 8 demonstrates a size effect for a 2D spin array (figure 3(b)): temperature dependence of B_c for the structures consisting of $N = 100$ (black circles) and $N = 12$ spins (white circles). One can clearly see the presence of the size effect in the 2D case, in contrast with the 1D one (figure 5). The system of $N = 12$ spins exhibits FM behavior up to 2.4 K, while the array of $N = 100$ spins—up to 4.5 K. To explain the existence of the size effect in the 2D case we note that the blocking temperature is determined mainly by the strength of exchange interaction of a spin with the neighboring units, i.e. (at a certain J) by the number of neighboring spins. The average number of neighboring spins N_{av} in the system of $N = 12$ units is 3.8, while $N_{av} = 5.2$ for $N = 100$. The difference in N_{av} leads to different blocking temperatures in the systems of 12 and 100 spins. In the 1D case the size effect is not pronounced (figure 5), since there is no noticeable increase of N_{av} with increasing N: $N_{av} = 1.80$ for $N = 10$ and $N_{av} = 1.98$ for $N = 100$.

Figure 9 shows the dependence of coercive field B_c for a 2D array of $N = 100$ spins on the MAE K and exchange constant J. The temperature of the system is $T = 0.5$ K. The FM behavior is seen for the whole range of values J and K involved in our study.
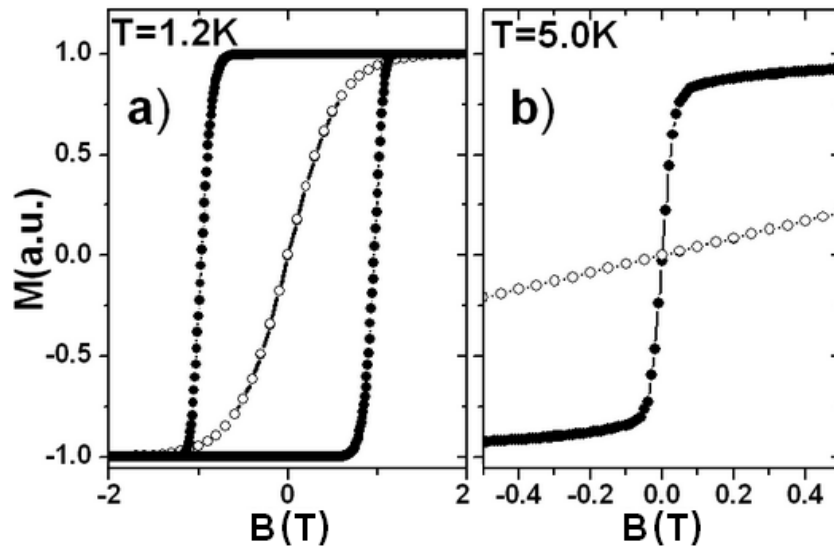
Figure 7. Magnetization response to the external magnetic field for the 2D hexagonal-ordered array of $N = 100$ spins at two temperatures: (a) 1.2 K, (b) 5.0 K. Black circles correspond to the following parameters of the Hamiltonian (1): $K = 1.0$ meV, $J = -0.3$ meV and $\mu = 3.2\mu_B$, while white circles correspond to: $K = 1.0$ meV, $J = 0$ meV and $\mu = 3.2\mu_B$.
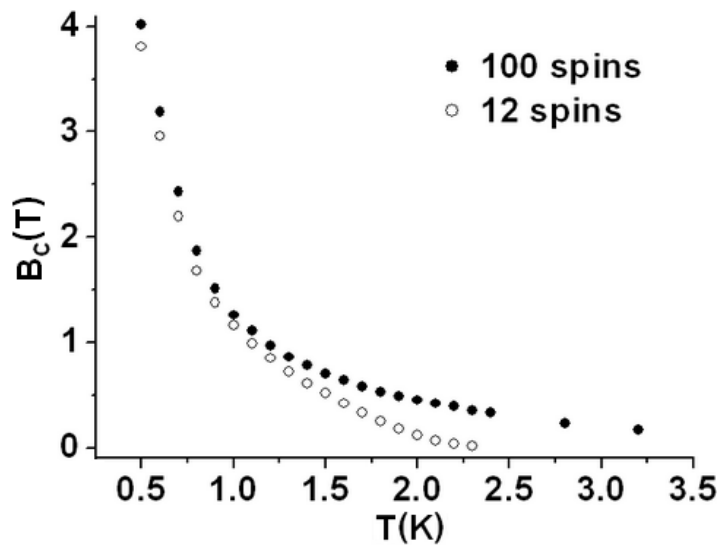
Figure 8. Temperature dependence of coercive field B_c for 2D hexagonal-ordered arrays of $N = 12$ and 100 spins. The parameters of the Hamiltonian (1) are: $K = 1.0$ meV, $J = -0.3$ meV and $\mu = 3.2\mu_B$.

It is of great importance to discuss the Kondo effect [69]–[73], which could arise in the considered class of the 1D and 2D systems (figure 2). In the Kondo effect, a localized magnetic moment of an adatom is screened below the Kondo temperature T_K and forms a correlated electron system with the surrounding conduction electrons on the non-magnetic host [69]–[73].
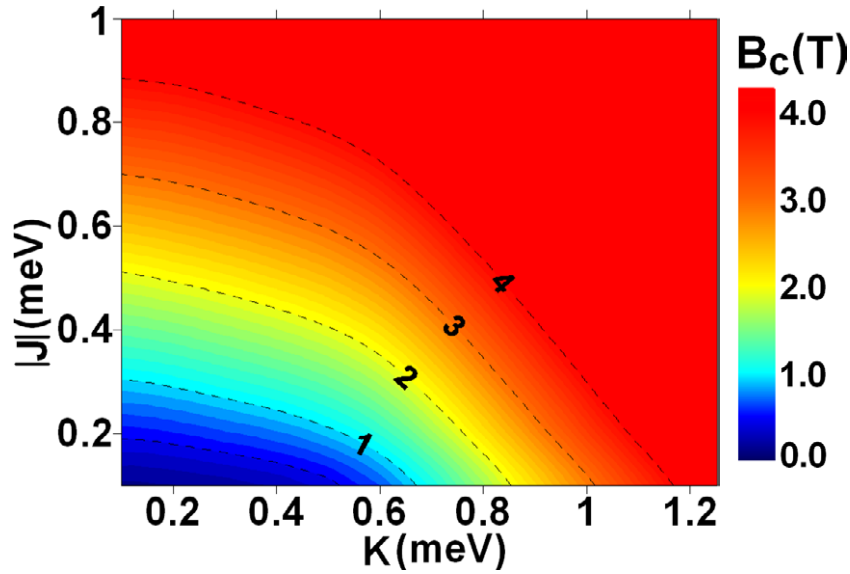
Figure 9. Dependence of coercive field B_c for a 2D hexagonal-ordered array of $N = 100$ spins on the MAE K and exchange coupling constant J. The diagram is obtained for $T = 0.5$ K. Dashed curves represent the equipotential lines of coercive field B_c of the corresponding magnitude (see thermometer).

Exchange interaction between adatoms can modify the Kondo temperature considerably [74]. Generally, if the magnetic ordering temperature T_m of a system of the FM-coupled units is larger than T_K, the observation of FM response is possible only in the temperature range (T_K, T_m) [74, 75]. Since the typical temperature of magnetic ordering T_m in the considered class of nanostructures is a few K, we note that all our conclusions are applicable to the systems that exhibit very small Kondo temperatures. Our results are also valid for the case of an underscreened Kondo lattice, when the coexistence of FM order and Kondo behavior is possible [76].

It is also worth noting that at low temperatures quantum effects (a spin switching induced by quantum tunneling (QT)) could play an important role [9]. In the following we discuss a possible effect of QT on the onset of ferromagnetism of spin chains and hexagonal-ordered 2D spin arrays. We suggest that the frequency of spin flips of an isolated adatom in the presence of QT can be described using the formula: $v = v_1 + v_0 \exp(-K/k_B T)$. Here, v_1 is the rate of spin switching induced by QT (it is independent of the temperature[7]) and $v_0 \exp(-K/k_B T)$ is the frequency of thermoactivated spin flips. If T is high enough, the second term dominates, and the frequency of spin flips follows the Arrhenius law. However, at low T, the term $v_0 \exp(-K/k_B T)$ tends exponentially to zero, and there is a range of temperatures where v_1 dominates, i.e. $v \simeq v_1$.

Let us consider an individual spin in the absence of external magnetic field. The Hamiltonian of such a system is $H = -K(s_z)^2$, independently of the absence or presence of QT.

---

[7] The spin flip due to quantum tunneling is temperature independent. This has been demonstrated by the theoretical calculations [77] and experimental studies [78, 79]. Later on, the same phenomenon has been observed for adatom diffusion on surfaces [80]–[82].
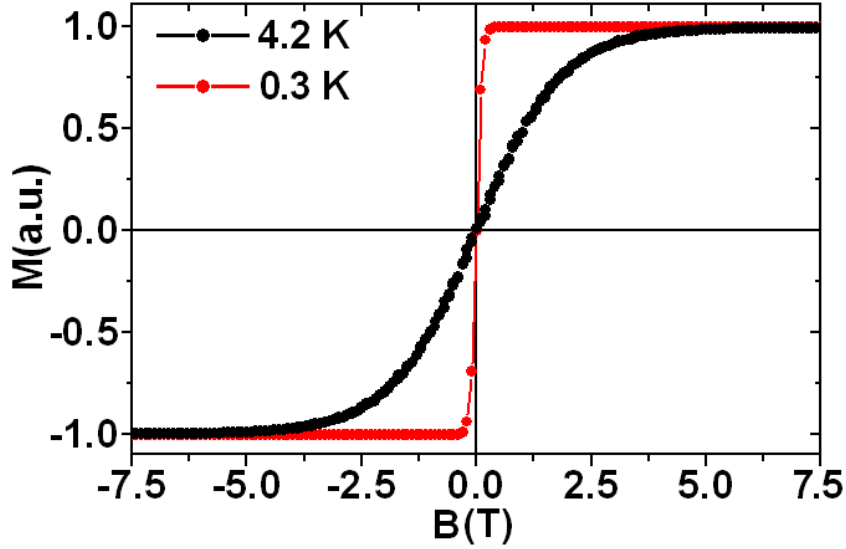
Figure 10. Magnetization response for a single Co adatom on Pt(111) at 0.3 and 4.2 K. The following parameters are used for simulations: $v_1 = 10^4$ Hz, $K = 9.3$ meV, $\mu = 3.8\mu_B$, $B_0 = 7.5$ T and $dB/dt = 0.01$ T s^{-1}.

The activation barrier K derived from this Hamiltonian sets the switching rate in the absence of QT: $v = v_0 \exp(-K/k_B T)$. The frequency of spin flips in the presence of QT can be written in the similar form: $v = [v_1 \exp(K/k_B T) + v_0]\exp(-K/k_B T)$. Since the Hamiltonian in both cases is the same, one can consider

$$v_{eff} = v_0 + v_1 \exp(K/k_B T) \tag{5}$$

as a new 'effective' prefactor instead of v_0 (see equation (3)) for the calculation of switching rate in the presence of QT in the framework of the applied kMC algorithm [19].

Let us now discuss possible values of v_1. The upper limit of v_1 is set by the condition $v_1 \ll v_0$, which is derived from the fact that at high T ($T \to \infty$) the frequency of thermoactivated spin flips v_0 is much larger than the frequency of spin flips promoted by QT. Therefore, $v_1 \ll 10^9$ Hz. The rough estimation of the lower limit of v_1 can be obtained from the experimental studies of Meier *et al* [9] on the magnetization response of individual Co adatoms placed on a Pt(111) surface. The S-like paramagnetic curves over Co adatoms on Pt(111) have been recorded at two different temperatures, 0.3 and 4.2 K [9]. It is well known that a Co adatom on Pt(111) has MAE $K = 9.3$ meV [6, 9]. From the formula $1/t_{av} \sim v_0\exp(-K/k_B T)$ (where t_{av} is the average time of a thermoactivated spin flip), one finds that $t_{av} = 10^{147}$ s at $T = 0.3$ K and $t_{av} = 10^2$ s at $T = 4.2$ K. At the same time, Meier *et al* [9] have reported that spin switching takes place much faster than the resolution time of the experiment (100 Hz). Hence the observed value of t_{av} is $\ll 0.01$ s. It has been suggested that either QT or current-induced magnetization switching could promote 'fast' spin flips of individual Co adatoms [9]. If we suggest that QT is responsible for the observed spin switching, we obtain the lower limit of $v_1 \gg 10^2$ Hz. As a result, we conclude that most probably v_1 is in the range between 10^4 and 10^7 Hz.

In order to take into account quantum effects, we have modified the kMC model described in section 2. The procedure of calculation of activation barriers remains unchanged; however,
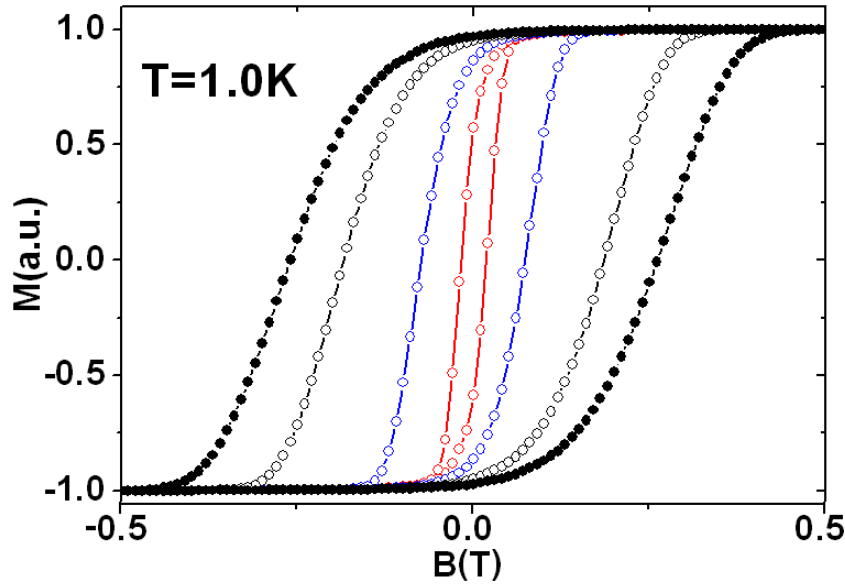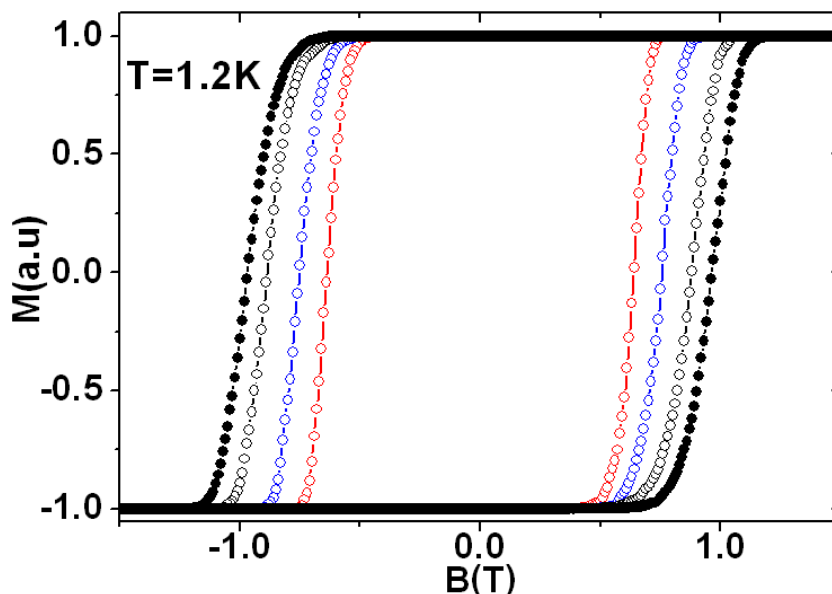
Figure 11. Effect of QT on the magnetization response for the 1D chain of $N = 100$ spins at $T = 1.0$ K. Black circles correspond to $v_1 = 0$ (absence of QT), white circles to $v_1 = 10^4$ Hz, blue circles to $v_1 = 10^5$ Hz and red circles to $v_1 = 10^6$ Hz. The values of the parameters of the Hamiltonian (1): $K = 1.0$ meV, $J = -0.3$ meV and $\mu = 3.2\mu_B$.

we employ prefactor v_{eff} (see equation (5)) instead of v_0 to compute transition rates (see equation (3)). To illustrate the concept of v_{eff}, firstly we have followed the experimental setup of Meier *et al* [9] on the magnetization response of individual Co adatoms on Pt(111) at the temperatures 0.3 and 4.2 K. The following values of parameters have been used in our calculations: $K = 9.3$ meV, $\mu = 3.8\mu_B$, $B_0 = 7.5$ T and $dB/dt = 0.01$ T s^{-1} (slow sweeping rate). The results of kMC simulations are presented in figure 10. For the calculations we have considered that $v_1 = 10^4$ Hz. We have also tested other magnitudes of v_1 within the range from 10^4 to 10^7 Hz and we have found that both the resulting curves remain unchanged. From figure 10 one can see that the magnetization response at both temperatures is paramagnetic. The values of saturation fields are about 0.3 T at 0.3 K and about 5.0 T at 4.2 K, in agreement with the experimental observations [9].

We now turn to the effect of QT on the possible onset of ferromagnetism in 1D spin chains and 2D hexagonal-ordered spin arrays at low temperatures. Figure 11 demonstrates the magnetization response for a chain of $N = 100$ spins at $T = 1.0$ K. We have already found (figure 4(a)) that this system exhibits FM behavior with coercive field $B_c = 0.26$ T (black circles in figure 11). White circles represent the magnetic signal calculated at $v_1 = 10^4$ Hz: FM response with $B_c = 0.18$ T. In the case of $v_1 = 10^5$ Hz (blue circles), we find that $B_c = 0.07$ T. Red circles demonstrate the magnetization response at $v_1 = 10^6$ Hz: hysteresis loop with $B_c = 0.02$ T is observed. If $v_1 = 10^7$ Hz, then $B_c = 0.003$ T (not shown in figure 11). Taking into account the results shown in figure 11, we conclude that QT could decrease the coercive field B_c. However, it does not influence the onset of ferromagnetism in 1D spin arrays.

We have also investigated the effect of QT on the magnetic behavior of the 2D array of $N = 100$ spins at $T = 1.2$ K (figure 12). Black circles demonstrate the hysteresis loop obtained

Figure 12. Effect of QT on the magnetization response for the 2D hexagonal-ordered array of $N = 100$ spins at $T = 1.2$ K. Black circles correspond to $v_1 = 0$ (absence of QT), white circles to $v_1 = 10^5$ Hz, blue circles to $v_1 = 10^6$ Hz and red circles to $v_1 = 10^7$ Hz. The values of the parameters of the Hamiltonian (1): $K = 1.0$ meV, $J = -0.3$ meV and $\mu = 3.2\mu_B$.

in the absence of QT ($v_1 = 0$): the system exhibits FM behavior with $B_c = 0.96$ T (see also figure 7(a)). At $v_1 = 10^4$ Hz the magnetization response is almost the same as that in the absence of QT, i.e. at $v_1 = 0$. The magnitude of the coercive field in this case is 0.95 T (not shown in figure 12). White circles (figure 12) demonstrate the magnetic signal at $v_1 = 10^5$ Hz: hysteresis loop with $B_c = 0.89$ T is observed. At $v_1 = 10^6$ Hz we find that $B_c = 0.76$ T (blue circles), whereas at $v_1 = 10^7$ Hz B_c is decreased to 0.64 T (red circles). Thus, similar to the 1D spin chains (see figure 11), the presence of QT does not affect the onset of ferromagnetism in 2D spin arrays.

4. Conclusion

Using the Heisenberg Hamiltonian, we have theoretically studied the magnetic properties of 1D and 2D spin systems with the parameters (exchange coupling constant and MAE), which are typical for atomic-scale structures stabilized by the substrate-mediated interaction. Our investigation has been performed by means of kinetic Monte Carlo simulations based on transition-state theory. We have shown that in the externally applied magnetic field at low temperatures (typically at 1–3 K), the considered class of spin systems exhibits hysteresis-like behavior. We have found that in the 2D hexagonal-ordered spin arrays the magnetization response depends on the size of the system, whereas in the 1D case the size-effect is not strong. Our systematic studies have demonstrated that QT does not influence the possible onset of ferromagnetism.

IOP Institute of Physics ⬤ DEUTSCHE PHYSIKALISCHE GESELLSCHAFT

Acknowledgments

References

[1] Barth J V, Costantini G and Kern K 2005 *Nature* **437** 671
[2] Himspel F J, Ortega J E, Mankey G J and Willis R F 1998 *Adv. Phys.* **47** 511
[3] Lu C L, Freeman A J and Oguchi T 1985 *Phys. Rev. Lett.* **54** 2700
[4] Stepanyuk V S, Hergert W, Wildberger K, Zeller R and Dederichs P H 1996 *Phys. Rev.* B **53** 2121
[5] Nonas B, Cabria I, Zeller R, Dederichs P H, Huhne T and Ebert H 2001 *Phys. Rev. Lett.* **86** 2146
[6] Gambardella P *et al* 2003 *Science* **300** 1130
[7] Gambardella P, Rusponi S, Cren T, Weiss N and Brune H 2005 *C. R. Phys.* **6** 75
[8] Hirjibehedin C F, Lin C-Y, Otte A F, Ternes M, Lutz C P, Jones B A and Heinrich A J 2007 *Science* **317** 1199
[9] Meier F, Zhou L, Wiebe J and Wiesendanger R 2008 *Science* **320** 82
[10] Gambardella P, Dallmeyer A, Maiti K, Malagoli M C, Eberhardt W, Kern K and Carbone C 2002 *Nature* **416** 301
[11] Shen J, Pierce J P, Plummer E W and Kirschner J 2003 *J. Phys.: Condens. Matter* **15** R1
[12] Hillenkamp M, Di Domenicantonio G and Félix C 2008 *Phys. Rev.* B **77** 014422
[13] Elmers H J, Hauschild J, Höche H, Gradmann U, Bethge H, Heuer D and Köhler U 1994 *Phys. Rev. Lett.* **73** 898
[14] Shen J, Skomski R, Klaua M, Jenniches H, Manoharan S S and Kirschner J 1997 *Phys. Rev.* B **56** 2340
[15] Brown G, Lee H K, Schulthess T C, Ujfalussy B, Stocks G M, Butler W H, Landau D P, Pierce J P, Shen J and Kirschner J 2002 *J. Appl. Phys.* **91** 7056
[16] Yan L, Przybylski M, Lu Y F, Wang W H, Barthel J and Kirschner J 2005 *Appl. Phys. Lett.* **86** 102503
[17] Shiraki S, Fujisawa H, Nakamura T, Muro T, Nantoh M and Kawai M 2008 *Phys. Rev.* B **78** 115428
[18] Gambardella P 2003 *J. Phys.: Condens. Matter* **15** 2533
[19] Li Y and Liu B-G 2006 *Phys. Rev.* B **73** 174418
[20] Dorantes-Dávila J and Pastor G M 1998 *Phys. Rev. Lett.* **81** 208
[21] Spisak D and Hafner J 2002 *Phys. Rev.* B **65** 235405
[22] Fruchart O, Klaua M, Barthel J and Kirschner J 1999 *Phys. Rev. Lett.* **83** 2769
[23] Qiang Y, Sabiryanov R F, Jaswal S S, Liu Y, Haberland H and Sellmyer D J 2002 *Phys. Rev.* B **66** 064404
[24] Pierce J P, Torija M A, Gai Z, Shi J, Schulthess T C, Farnan G A, Wendelken J F, Plummer E W and Shen J 2004 *Phys. Rev. Lett.* **92** 237201
[25] Torija M A, Li A P, Guan X C, Plummer E W and Shen J 2005 *Phys. Rev. Lett.* **93** 257203
[26] Rohart S, Repain V, Tejeda A, Ohresser P, Scheurer F, Bencok P, Ferrer J and Rousset S 2006 *Phys. Rev.* B **73** 165412
[27] Skomski R, Zhang J, Sessi V, Honolka J, Enders A and Kern K 2008 *J. Appl. Phys.* **103** 07D519
[28] Poulopoulos P, Jensen P J, Ney A, Lindner J and Baberschke K 2002 *Phys. Rev.* B **65** 064431
[29] Hernando A, Briones F, Cebollada A and Crespo P 2002 *Physica* B **322** 318
[30] Zhou J, Skomski R and Sellmyer D J 2006 *J. Appl. Phys.* **99** 08F909
[31] Einstein T L and Schrieffer J R 1973 *Phys. Rev.* B **7** 3629
[32] Lau K H and Kohn W 1978 *Surf. Sci.* **75** 69
[33] Hyldgaard P and Persson M 2000 *J. Phys.: Condens. Matter.* **12** L13
[34] Brune H, Wintterlin J, Ertl G and Behm R J 1990 *Europhys. Lett.* **13** 123
[35] Crommie M F, Lutz C P and Eigler D M 1993 *Science* **262** 218
[36] Crommie M F, Lutz C P and Eigler D M 1993 *Nature* **363** 524

[37] Li J, Schneider W-D, Berndt R and Crampin S 1998 *Phys. Rev. Lett.* **80** 3332
[38] Bürgi L, Jeandupeux O, Hirstein A, Brune H and Kern K 1998 *Phys. Rev. Lett.* **81** 5370
[39] Braun K-F and Rieder K-H 2002 *Phys. Rev. Lett.* **88** 096801
[40] Pivetta M, Silly F, Patthey F, Pelz J P and Schneider W-D 2003 *Phys. Rev.* B **67** 193402
[41] Stepanyuk V S, Baranov A N, Tsivlin D V, Hergert W, Bruno P, Knorr N, Schneider M A and Kern K 2003 *Phys. Rev.* B **68** 205410
[42] Negulyaev N N, Stepanyuk V S, Niebergall L, Bruno P, Hergert W, Repp J, Rieder K-H and Meyer G 2008 *Phys. Rev. Lett.* **101** 226601
[43] Bürgi L, Knorr N, Brune H, Schneider M A and Kern K 2002 *Appl. Phys.* A **75** 141
[44] Lau K H and Kohn W 1977 *Surf. Sci.* **65** 607
[45] Longo R C, Stepanyuk V S and Kirschner J 2006 *J. Phys.: Condens. Matter* **18** 9143
[46] Repp J, Moresco F, Meyer G, Rieder K-H, Hyldgaard P and Persson M 2000 *Phys. Rev. Lett.* **85** 2981
[47] Knorr N, Brune H, Epple M, Hirstein A, Schneider M A and Kern K 2002 *Phys. Rev.* B **65** 115420
[48] Bogicevic A, Ovesson S, Hyldgaard P, Lundqvist B I, Brune H and Jennison D R 2000 *Phys. Rev. Lett.* **85** 1910
[49] Fichthorn K A and Scheffler M 2000 *Phys. Rev. Lett.* **84** 5371
[50] Fichthorn K A, Merrick M L and Scheffler M 2002 *Appl. Phys.* A **75** 17
[51] Fichthorn K A, Merrick M L and Scheffler M 2003 *Phys. Rev.* B **68** 041404
[52] Silly F, Pivetta M, Ternes M, Patthey F, Pelz J P and Schneider W-D 2004 *New J. Phys.* **6** 16
[53] Silly F, Pivetta M, Ternes M, Patthey F, Pelz J P and Schneider W-D 2004 *Phys. Rev. Lett.* **92** 016101
[54] Stepanyuk V S, Niebergall L, Longo R C, Hergert W and Bruno P 2004 *Phys. Rev.* B **70** 075414
[55] Rogowska J M and Maciejewski M 2006 *Phys. Rev.* B **74** 235402
[56] Hu J, Teng B, Wu F and Fang Y 2008 *New J. Phys.* **10** 023033
[57] Ternes M, Weber C, Pivetta M, Patthey F, Pelz J P, Giamarchi T, Mila F and Schneider W-D 2004 *Phys. Rev. Lett.* **93** 146805
[58] Negulyaev N N, Stepanyuk V S, Niebergall L, Hergert W, Fangohr H and Bruno P 2006 *Phys. Rev.* B **74** 035421
[59] Ziegler M, Kröger J, Berndt R, Filinov A and Bonitz M 2008 *Phys. Rev.* B **78** 245427
[60] Ding H F, Stepanyuk V S, Ignatiev P A, Negulyaev N N, Niebergall L, Wasniowska M, Gao C L, Bruno P and Kirschner J 2007 *Phys. Rev.* B **76** 033409
[61] Schiffrin A, Reichert J, Auwärter W, Jahnz G, Pennec Y, Weber-Bargioni A, Stepanyuk V S, Niebergall L, Bruno P and Barth J V 2008 *Phys. Rev.* B **78** 035424
[62] Liu C, Uchihashi T and Nakayama T 2008 *Phys. Rev. Lett.* **101** 146104
[63] Fichthorn K A and Weinberg W H 1991 *J. Chem. Phys.* **95** 1090
[64] Pick Š, Stepanyuk V S, Klavsyuk A L, Niebergall L, Hergert W, Kirschner J and Bruno P 2004 *Phys. Rev.* B **70** 224419
[65] Lazarovits B, Szunyogh L and Weinberger P 2006 *Phys. Rev.* B **73** 045430
[66] Lounis S, Mavropoulos P, Dederichs P H and Blügel S 2006 *Phys. Rev.* B **73** 195421
[67] Vindigni A, Rettori A, Pini M G, Carbone C and Gambardella P 2006 *Appl. Phys.* A **82** 385
[68] Glauber R J 1963 *J. Math. Phys.* **4** 294
[69] Li J, Schneider W-D, Berndt R and Delley B 1998 *Phys. Rev. Lett.* **80** 2893
[70] Madhavan V, Chen W, Jamneala T, Crommie M F and Wingreen N S 1998 *Science* **280** 567
[71] Wahl P, Diekhöner L, Schneider M A, Vitali L, Wittich G and Kern K 2004 *Phys. Rev. Lett.* **93** 176603
[72] Otte A F, Ternes M, von Bergmann K, Loth S, Brune H, Lutz C P, Hirjibehedin C F and Heinrich A J 2008 *Nat. Phys.* **4** 847
[73] Ternes M, Heinrich A J and Schneider W-D 2009 *J. Phys.: Condens. Matter* **21** 053001
[74] Wahl P, Simon P, Diekhöner L, Stepanyuk V S, Bruno P, Schneider M A and Kern K 2007 *Phys. Rev. Lett.* **98** 056601

IOP Institute of Physics ⚽DEUTSCHE PHYSIKALISCHE GESELLSCHAFT

[75] Lee W H, Shelton R N, Dhar S K and Gschneider K A 1987 *Phys. Rev.* B **35** 8523

[76] Perkins N B, Iglesias J R, Núñez-Regueiro M D and Coqblin B 2007 *Europhys. Lett.* **79** 57006

[77] Chudnovsky E M and Gunther L 1988 *Phys. Rev. Lett.* **60** 661

[78] Friedman J R, Sarachik M P, Tejada J and Ziolo R 1996 *Phys. Rev. Lett.* **76** 3830

[79] Thomas L, Lionti F, Ballou R, Gatteschi D, Sessoli R and Barbara B 1996 *Nature* **383** 145

[80] Lauhon L J and Ho W 2000 *Phys. Rev. Lett.* **85** 4566

[81] Repp J, Meyer G, Rieder K-H and Hyldgaard P 2003 *Phys. Rev. Lett.* **91** 206102

[82] Gadzuk J W 2006 *Phys. Rev.* B **73** 085401